IOP Publishing
Superconductor Science and Technology
Supercond. Sci. Technol. **33** (2020) 105011 (13pp)
https://doi.org/10.1088/1361-6668/abaec2

Quench detection using Hall sensors in high-temperature superconducting CORC®-based cable-in-conduit-conductors for fusion applications

J D Weiss[1,2], **R Teyber**[3], **M Marchevsky**[3] **and D C van der Laan**[1,2]

[1] University of Colorado Boulder, Boulder, CO 80309, United States of America
[2] Advanced Conductor Technologies LLC, Boulder, CO 80301, United States of America
[3] Lawrence Berkeley National Laboratory, Berkeley, California 94720, United States of America

E-mail: Jeremy.weiss@colorado.edu

Received 27 May 2020, revised 29 July 2020
Accepted for publication 12 August 2020
Published 2 September 2020

Abstract
Advanced magnet systems for fusion applications would greatly benefit from the use of high-temperature superconductors (HTS). These materials allow fusion magnets to operate at higher magnetic fields, allowing for more compact fusion machines, and allow for operation at elevated temperatures, enabling demountable coils that provide access for maintenance of the fusion reactor. Quench detection remains a major challenge in the protection of HTS magnets that are vulnerable to localized conductor burnout due to their low quench propagation velocities. One of the methods explored is the use of Hall sensors that are incorporated in or near the magnet terminations that can detect local field variations that occur as a result of current redistribution within the conductor to bypass a hotspot within the magnet winding. This method is potentially well suited for Cable in Conduit Conductors, such as those made from Conductor on Round Core (CORC) cables, in which sub-cables containing HTS tapes are connected to the terminations at a low resistance. To demonstrate the technique, a CORC® triplet consisting of three sub-cables, rated for 4 kA operation at 77 K, was manufactured and Hall sensors were used to measure local field variations next to the terminations due to current redistribution between the cables. The Hall response was compared to voltages that developed over the cables and terminations as a local hotspot was applied to different cables in the triplet. It was found that the Hall sensors were faster and more sensitive than voltage contact measurements and were able to reliably detect current redistribution of only a few amperes caused by a hotspot, well before the triplet exceeded its critical current. The method also allowed the detection of heater-induced hotspots during high ramp rates of 2 kA s^{-1} relevant for fusion applications. Hall sensors have a distinct benefit of being less sensitive to inductive pickup of AC interference compared to voltage contact measurements that make quench detection through voltage measurements in magnets especially challenging. The method can also be used for diagnostic measurements of current redistribution caused by other sources such as inhomogeneous current injection from faulty joints, or localized conductor damage. The Hall sensors are likely capable of detecting the onset of a quench that may occur a far

distance away from the sensor location, presenting a breakthrough in HTS quench detection that potentially removes one of the remaining barriers to reliable operation of large HTS magnet systems.

Keywords: CORC®, HTS cable, REBCO, quench, Hall sensor, fusion magnet, CICC

(Some figures may appear in colour only in the online journal)

1. Introduction

High-temperature superconductors (HTS) such as RE-$Ba_2Ca_3O_{7-\delta}$ (REBCO, RE = rare earth) coated conductors are an enabling technology for the next generation of compact fusion machines [1–3] and high-field accelerator magnets [4, 5] that could operate at magnetic fields (B) exceeding 20 T. The present state-of-the-art superconducting magnets for fusion such as the international thermal-nuclear reactor (ITER) are based on low-temperature superconductors (LTS) that are limited in performance to a magnetic field far below 20 T at conductor operating temperatures of less than a few Kelvin. The plasma volume needed to produce net positive energy output scales with B^3 [6], with LTS-based fusion machines requiring substantial volume and therefore costs to develop [1, 2, 7, 8]. High-field operation of HTS presents an opportunity to make future fusion devices much more compact, potentially reducing the construction time and device cost significantly. While operation at elevated temperatures of 20–30 K reduces cooling costs, it also enables toroidal field (TF) coils with demountable joints that would allow convenient access to the fusion device interior for maintenance [2, 8, 9].

Magnets for fusion devices require high currents to operate at low inductances because of their large size and need to be ramped quickly, both to charge (central solenoid) and dynamically shape (poloidal field coils) the plasma. This is practically achieved by using conductors with very high operating currents of several 10's of kA. To achieve such currents using REBCO coated conductors, many tapes must be combined or cabled together. Several REBCO cabling approaches are currently being developed including Conductor on Round Core (CORC®) [10–12], Twisted Stacked-Tape Cable (TSTC) [13, 14], and Roebel conductors [15]. Multiple fusion cable designs incorporating bundled stacks of REBCO tapes have been developed, including efforts at the Paul Scherrer Institute (PSI) [16, 17], ENEA [18, 19], the CroCo cable design at Karlsruhe Institute of Technology [20, 21] and the STARS conductor at the National Institute for Fusion Science in Japan [9, 22]. CORC® Cable in Conduit Conductors (CICC) are also being developed to allow operating currents exceeding 50–80 kA at 10–20 T magnets [23, 24].

One of the technical challenges of safely operating large HTS magnets is the much lower quench propagation velocity in HTS conductors, compared to LTS from which conventional magnet systems are currently made [25–27]. When a normal zone develops in HTS, the dissipation remains localized and is thus more difficult to detect with conventional voltage measurements than in LTS magnets where the hotspot propagates quickly. If a normal zone is not detected in time it will lead to the burnout of the magnet system. Fast and reliable quench detection is thus essential for safe magnet operation. The development of quench detection and protection methods tailored to HTS are naturally the next important steps to produce reliable HTS fusion magnet technology. In the context of this paper, the term quench detection refers to detecting the superconducting-to-normal transition of any portion of the superconducting cable.

Several methods are currently being explored for quench detection in HTS magnets, including Rayleigh scattering in optical fibers [28, 29], stray capacitance monitoring [30], and diffuse ultrasound thermometry [31]. While many of these techniques are promising, none have demonstrated real-time quench protection with the same efficacy and ease-of-use as traditional voltage contact measurements in LTS magnets. Furthermore, many of the techniques, such as optical fibers and co-wound voltage taps, require incorporation within the magnet windings and can be affected by variation of strain or electromagnetic interference. This complicates their use in fusion magnets that will experience a wide range of current ramping conditions, high conductor strains, and various sources of background electromagnetic noise.

A potential breakthrough in quench detection within HTS magnet systems is the use of local magnetic field sensors [32–34], such as Hall sensors, to determine changes in current distribution between tapes in HTS cables caused by the development of a local hotspot at the onset of a magnet quench. This technique has already been demonstrated for slit HTS tapes and single CORC® cables [35–37]. Limited current sharing between tapes in CORC® cables in combination with low splice resistances between the tapes and cable terminations cause the majority of the current redistribution to occur within the terminations [38], where Hall sensors can be easily integrated. In contrast to measuring current redistribution within tapes of a single CORC® cable, arrays of Hall sensors are an extremely attractive quench detection method for use in CICC due to higher currents within the cables of CICC and limited current sharing between the cables in the CICC. Here, we compare the response of Hall sensors placed between the insulated CORC® cables in a CORC®-CICC to the response of voltage contacts when current approaches the critical current (I_c) and when a hotspot is induced by a local heater on one of the cables. The results show the

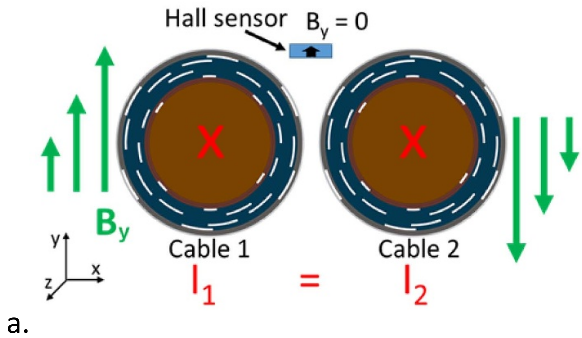

Figure 1. Overview showing current re-distribution between two CORC® cables and the vertical magnetic field component generated between the cables when the current balance changes due to appearance of resistance at a local hotspot in one of the cables. (a) Currents are balanced, and (b) currents are unbalanced.

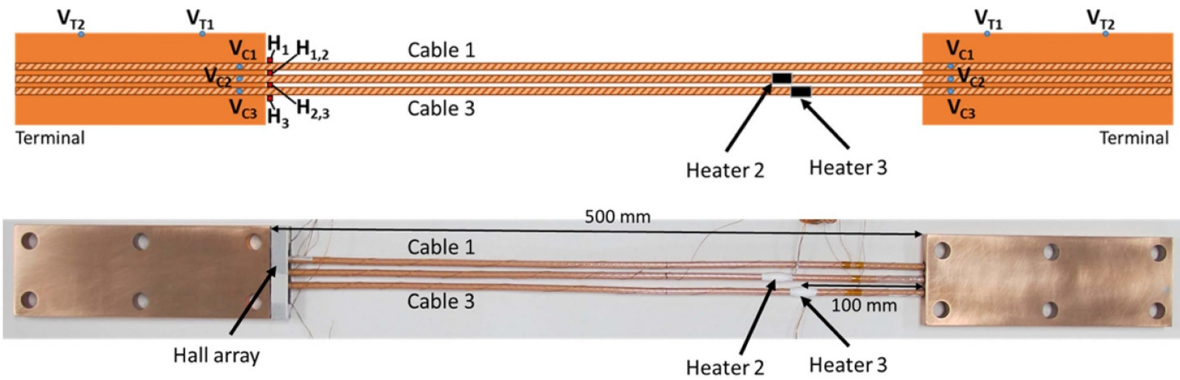

Figure 2. Schematic and picture of CORC® triplet sample including location of Hall sensors (H_1, $H_{1,2}$, $H_{2,3}$, H_3), voltage taps, and heaters.

effectiveness of the localized magnetic sensor measurements over conventional voltage measurements in CORC®-CICC, where Hall sensors were able to detect the onset of a quench sooner and with higher resolution than the voltage contacts.

2. Experimental methods

2.1. Quench detection in CICC using localized Hall sensors

In a superconducting state, and with equal contact resistance between the cables and the terminations, all sub-cables in a CICC carry approximately the same current, and therefore the superimposed field between parallel conducting paths tends to cancel out. For example, figure 1 shows the cross-section of two CORC® cables. The corresponding vertical field (B_y) components of the two currents in the neighbouring cables being measured by the Hall sensor are compensated because they are equal in magnitude and opposite in direction. As the critical current of one cable is reduced to below its operating current because of a local hotspot, current is redistributed into the other cable to keep the total current constant. Such redistribution produces an unbalanced vertical magnetic field between the cables, as shown in figure 1(b). This change in field is readily detectable with a 1D Hall sensor to measure B_y [35] placed at a convenient point in the middle line between the two cables, for instance near one of the current terminals. Hall sensors placed on the outside of the cable bundle can also detect current redistribution within the cables, as will be outlined in sections 3 and 4.

The scenario considered above works best when the cables are connected at the terminals with a very low-resistance joint while there is significantly higher resistance between the cables in the CICC. This is the case for most HTS CICC conductors being developed for fusion applications. Terminal and joint resistances of less than 5 nΩ (4.5 K, 4–9 T) have been measured in CORC®-CICC [39, 40] and TSTC-based CICC [41]. While CORC® inter-cable resistances have not been studied for any CICC layouts, the contact resistance between cables is expected to be relatively high since current would have to transverse several resistive layers to share current from one cable to another. The contact resistance between HTS tape bundles in one of the ENEA HTS CICC samples was 13 000 nΩm at 4.2 K [42], while inter-petal resistances for ITER CICC based on LTS conductors tend to be more than 200 nΩm and are optimized to control AC losses [43, 44]. Multiple Hall arrays along the length of a CICC would have to be applied for quench detection if the inter-strand resistance is much lower than the terminal resistance, such as would likely be the case for a completely solder filled CICC. The technique may be less applicable to CICC made from LTS as their low thermal stability can also lead to other magnetic instabilities that have been measured with local magnetic sensors [33, 34].

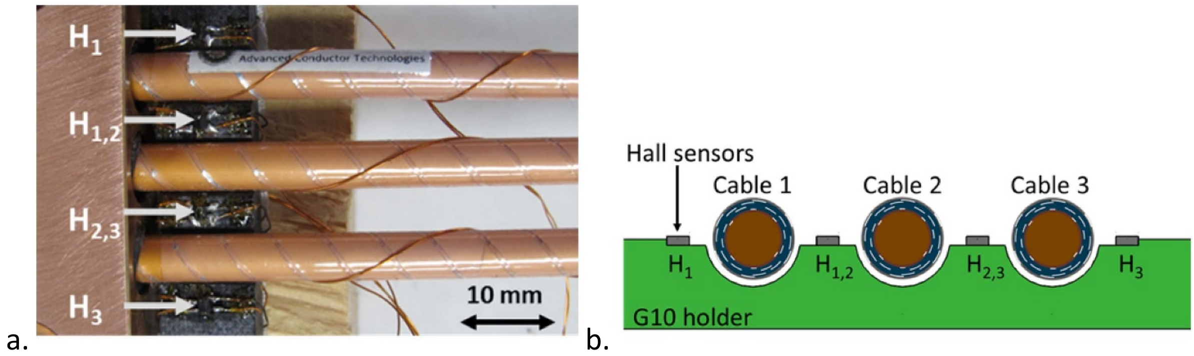

Figure 3. (a) Close-up of Hall array consisting of 4 sensors positioned besides the CORC® cables. (b) Overview of the transverse cross-section of the CORC® triplet, showing the location of the Hall sensors relative to CORC® cables.

2.2. Sample preparation

Three CORC® cables of 5.1 mm in diameter were arranged in a parallel configuration and terminated in two copper plates as shown in figure 2. The sample length was 500 mm between the terminations that each were 200 × 70 × 12 mm in size. The tape layers in the cables were tapered and soldered within the copper plates and current was injected into the samples from either side. Each cable contained a total of 12 SCS4050 tapes from SuperPower Inc. wound into 6 layers onto a 4.3 mm diameter solid copper core. The average tape I_c was 134 A at 77 K in self-field, resulting in a total I_c of about 4.8 kA for the CORC® triplet.

Four Hall sensors of type AKM HG-106 A (H_1, $H_{1,2}$, $H_{2,3}$, H_3) were positioned between the cables, next to one of the terminals, with a spacing of about 5 mm from the center of each CORC® cable as shown in figure 3. The Hall sensors were arranged in the same plane as the CORC® cables, measuring the out-of-plane component of the magnetic field. The sensors were powered in series using a 5 V power supply resulting in a room temperature transfer function of around 0.31–0.40 mV mT^{-1}. Wire heaters were wound around Cables 2 and 3 over a length of approximately 10 mm, at a distance of about 350–400 mm from the Hall array. Voltage wires were installed within the solder layer between each cable and termination to measure the voltage (V) over each CORC® cable (V_{C1}, V_{C2}, V_{C3}) as shown in figure 2. One wire from each voltage tap pair was guided back along the length of each cable before being twisted to minimize inductive pickup. Two pairs of voltage wires were also installed to measure the overall voltage between the terminals (V_{T1}, and V_{T2}). All experiments were carried out at 76 K which is the boiling point of nitrogen in Boulder, Colorado.

3. Results

3.1. Hall sensor and voltage response during constant current ramp rates

Baseline measurements were performed where voltage was measured as a function of current (V(I)) for various current ramp rates. Figure 4 shows the sample voltages compared to the Hall voltages (V_H) for current ramp rates of 20 A s^{-1} and 5000 A s^{-1}. Also plotted is the derivative of the Hall voltages that highlights when the Hall voltages deviate from linear behavior during the current ramp, which is a clear indication that current no is longer distributed evenly between the CORC® cables.

If current was evenly distributed in each cable of the triplet throughout the current ramp, the Hall measurements should be linear with current and the derivatives constant. Figure 4 shows that at approximately 1500–2000 A, Hall sensors $H_{2,3}$ and H_3 start to deviate from linear behavior, suggesting that current balance changes between the CORC® cables. This could be caused by a non-uniform contact resistance within the terminations or between the copper plates used to inject current. At about 3600–4000 A, the voltage over CORC® cable 3 begins to rise as it begins its superconducting-to-normal transition and an inflection point is observed in each Hall sensor response as the other two cables carry a larger fraction of the overall current. At about 4000 A, voltage begins to develop over the other two cables. These measurements show that the Hall sensor array is very well suited to monitor current distribution within a CICC, even in the absence of a quench.

3.2. Hall sensor and voltage tap response to a heater induced hotspot during constant current operation

Static heat pulse experiments were carried out on the CORC® triplet where current was ramped to a given value and held constant while heaters were then used to initiate a hotspot on either cable 2 or cable 3. Voltages across each CORC® cable and between terminations were monitored and compared to Hall sensor readings. Figures 5(a) and (c) show the voltage output of the Hall sensors and the voltage measured over the terminations when current was ramped to 3 kA and when a heat pulse was applied to cable 2 or 3, respectively, once the current plateau was reached. Current was then ramped back down to 0 A. With current equally distributed, the voltages of Hall sensors H_1 and H_3, as well as $H_{1,2}$ and $H_{2,3}$, should be equal and opposite at a given current. However, measured voltages tend to be shifted towards a positive value for all sensors. This could be an indicator of uneven current distribution or due to the limited Hall sensor positioning tolerance of

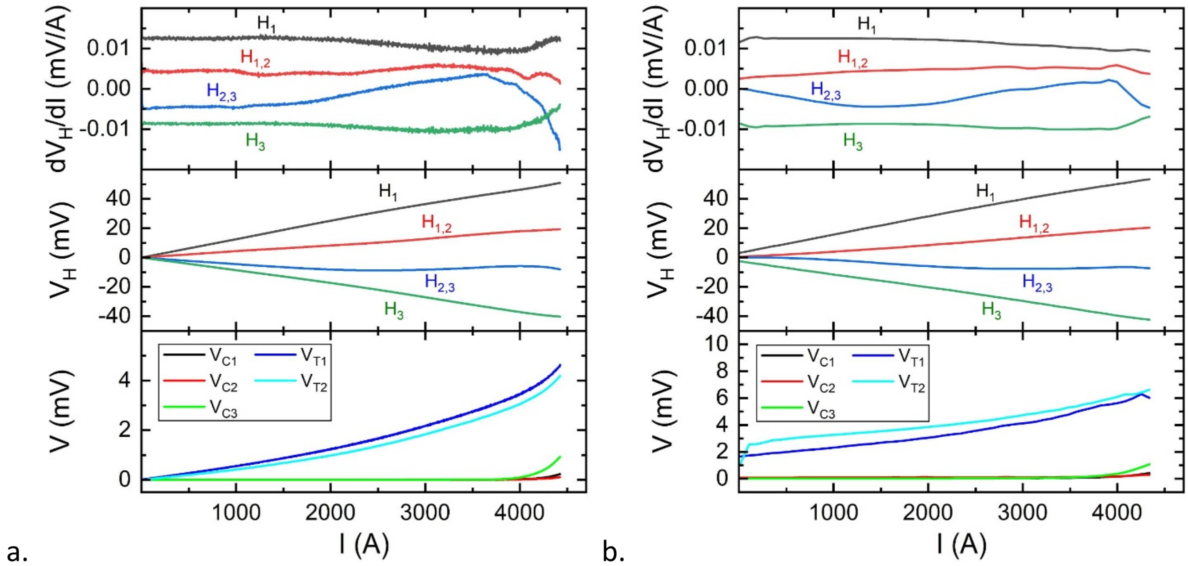

Figure 4. CORC® sample voltages (bottom), Hall voltages (middle), and derivative of Hall voltages (top) at 76 K as a function of current measured at current ramp rates of (a) 20 A s^{-1} and (b) 5000 A s^{-1}.

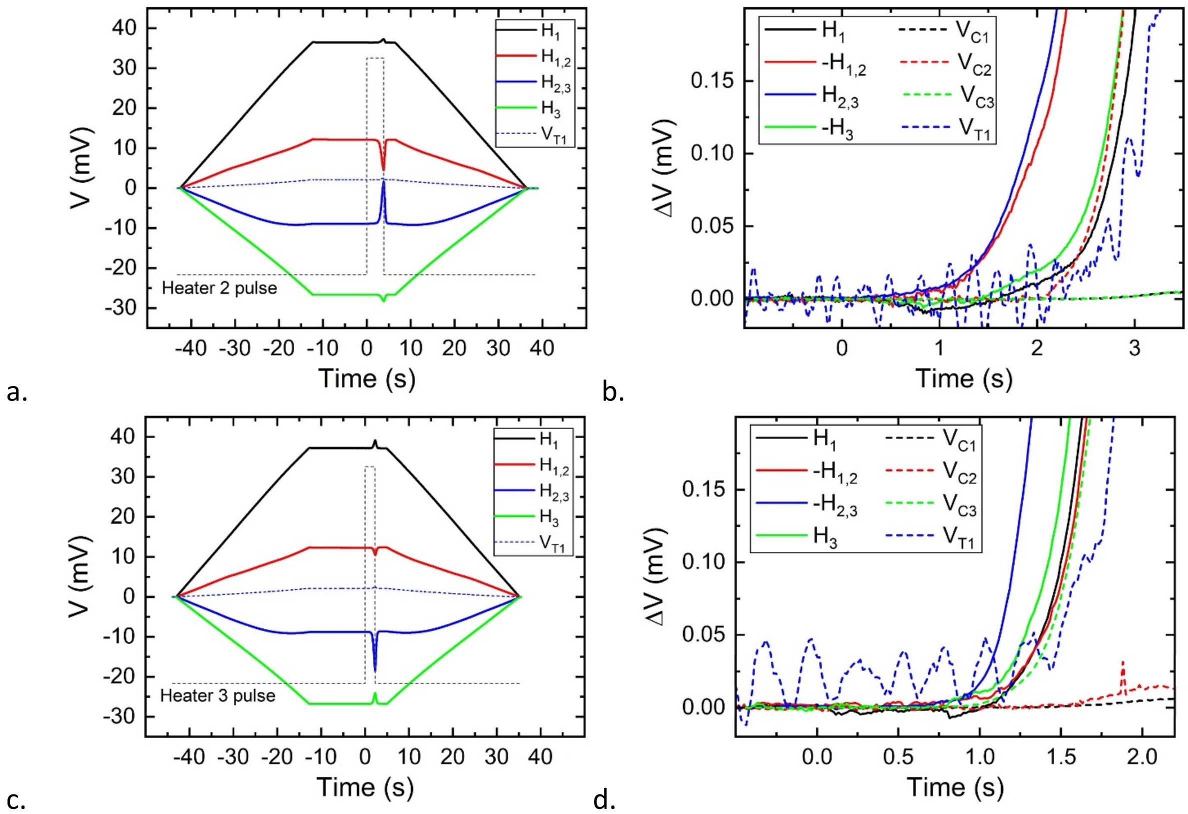

Figure 5. Hall sensor voltages and voltage over the terminations measured as a function of time at 76 K for a current ramp to 3000 A, followed by a 5 W heat pulse applied to (a) cable 2 and (c) cable 3. Current was then ramped back down. (b), (d) Comparison of voltages from (a) and (c), respectively, after subtracting the initial voltage measured before the heater pulse. Time = 0 corresponds to when the heater is turned on.

about 1 mm (see figure 3(b)), as will be discussed in section 4.

While the self-field of the cables results in a significant Hall signal that varies with current, the self-fields generated between adjacent cables are opposing, resulting in a lower field measured between cables (Hall sensors $H_{1,2}$ and $H_{2,3}$). A linear component that varies with current is also measured over the terminations (blue dotted lines in figures 5(a) and (c)), which is associated with their resistance, though the magnitude is much lower than the voltage output of the

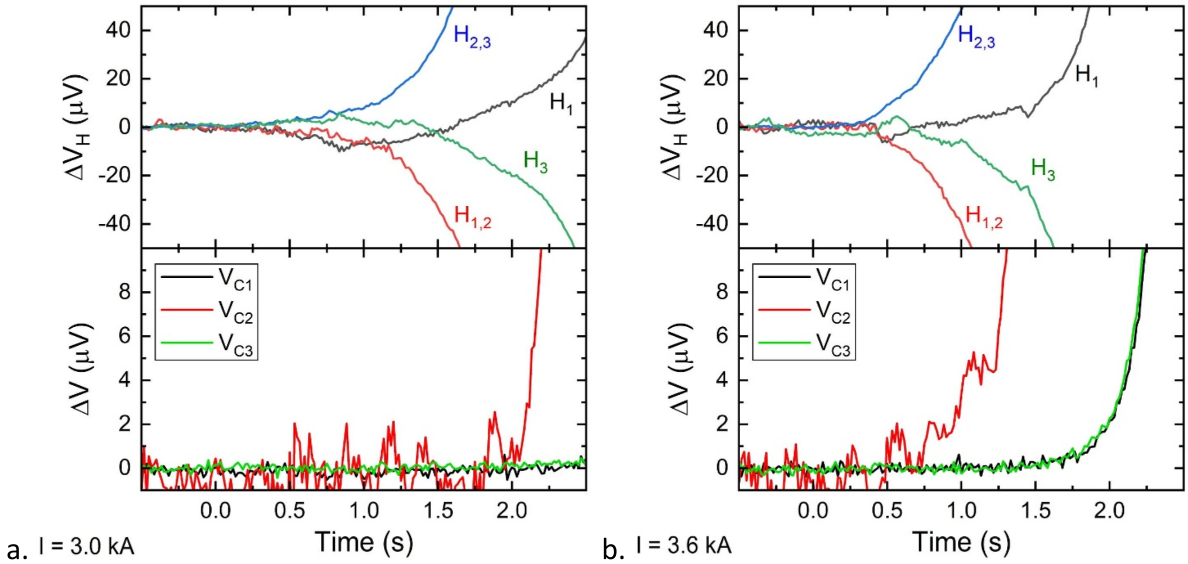

Figure 6. Change in Hall sensor voltage and voltage measured over the CORC® triplet at 76 K as a function of time, following a 5 W heat pulse applied to cable 2 at a constant current of (a) 3.0 kA and (b) 3.6 kA.

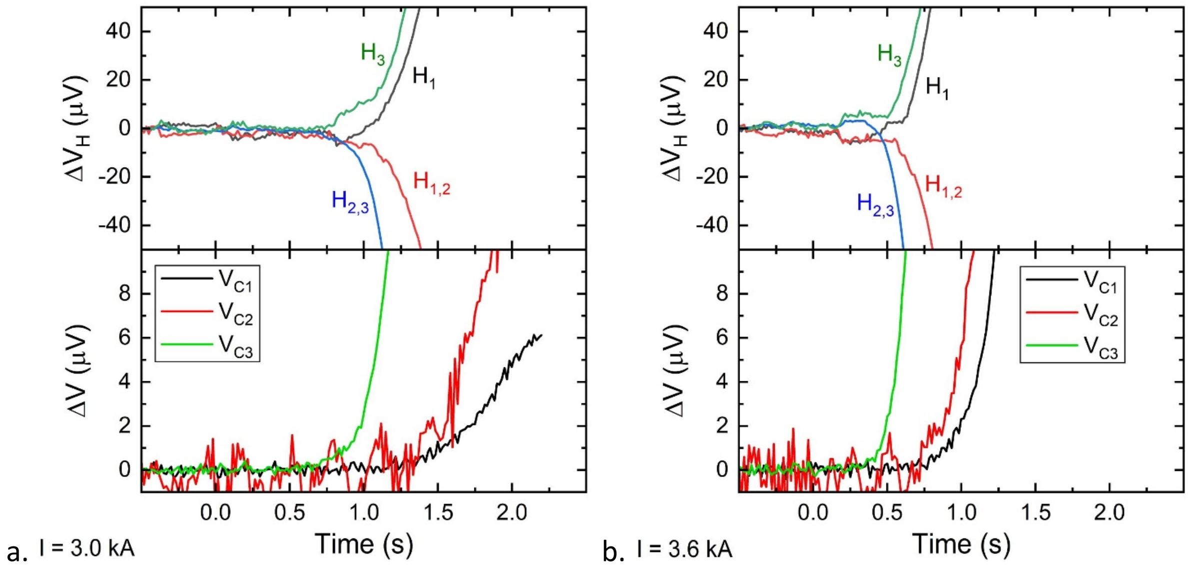

Figure 7. Change in Hall sensor voltage and voltage measured over the CORC® triplet at 76 K, as a function of time following a 5 W heat pulse applied to cable 3 at a constant current of (a) 3.0 kA and (b) 3.6 kA.

Hall sensors. In either case, it is relatively straightforward to subtract the initial voltage at constant current to obtain the change in voltage (ΔV). Figures 5(b) and (d) show a comparison of ΔV for Hall sensor and voltage tap measurements taken from the data shown in figures 5(a) and (c). In these figures, Time = 0 is when the heater is turned on. For clarity, all voltages are shown as a positive value. The Hall sensor voltage rise precedes that measured with the voltage contacts by about 0.2–0.5 s. In addition, the noise floor is 10 times lower for the Hall sensor measurements than for the voltage measured over the terminations, where significant inductive voltage noise remained. The tendency of the inductive voltage noise to increase with sample length is what makes quench detection using voltage contacts such a challenge in HTS coils.

Data is compared while focusing on the noise floor of each data set to explore the limitations of the Hall sensors compared to traditional voltage contacts to detect a quench in the CORC® triplet. It should be reiterated that great care was taken to minimize inductive pickup for the voltage measurements taken over the cables. For this short sample, it was thus possible to achieve a noise floor around 1 μV while I_c would be determined at 50 μV when using a 1 μV cm^{-1} voltage criterion and a 50 cm sample length. The voltage at which I_c is reached at the location of the hotspot is most likely much lower because the hotspot only covers a fraction of the conductor length.

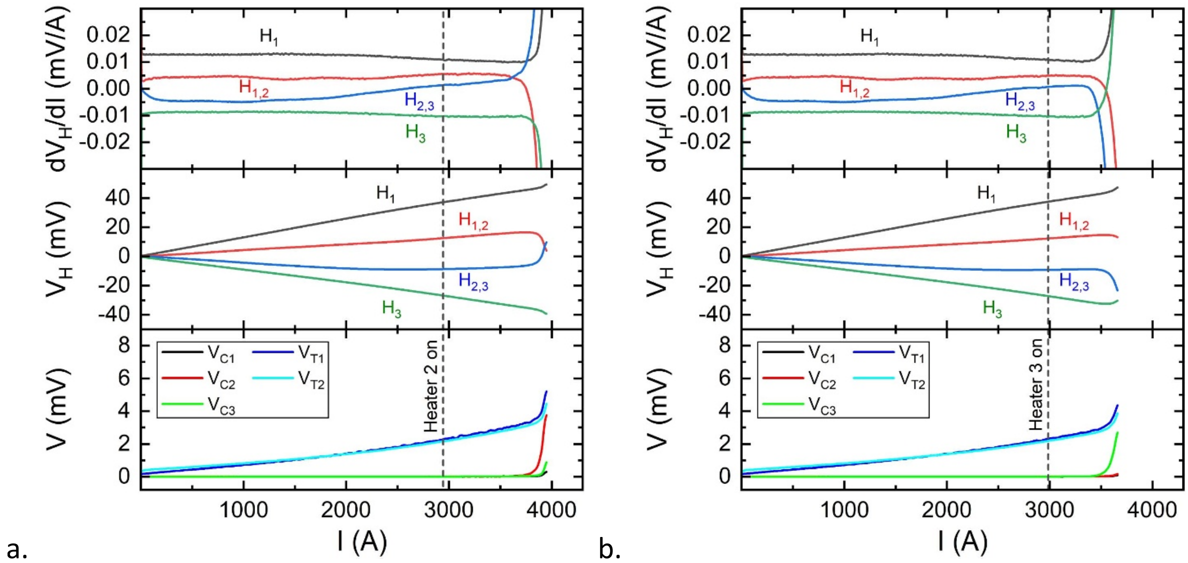

Figure 8. CORC® sample voltages (bottom), Hall voltages (middle), and derivatives of Hall voltages (top) as a function of current measured at 76 K at a current ramp rate of 500 A s^{-1} while a hotspot is initiated by applying a heater to (a) cable 2 and (b) cable 3.

The noise floor of the voltage measurement is independent of hotspot size and will likely scale with conductor length, highlighting the difficulty of detection a local hotspot in a long HTS conductor.

Figure 6 shows Hall sensor and voltage contact measurements as a function of time following a 5 W heater applied to the middle cable (cable 2) at two static currents: 3 kA, and 3.6 kA, corresponding to about 75%, and 90% of the sample I_c. These values were chosen to represent expected normal operating currents of the conductor considering margin. Figure 7 shows the same measurements repeated with a heater applied to one of the side cables (cable 3).

3.3. Hall sensor and voltage contact response to a heater induced hotspot during current ramping

Measurements were performed using heaters to initiate a hotspot on a given cable of the CORC® triplet while increasing current to determine whether the Hall array could be used to detect a quench while ramping current, as would be a frequent occurrence in fusion magnets. Figure 8 compares Hall sensor voltage and the voltage measured over the sample as a function of current ramped at 500 A s^{-1}, while a hotspot is initiated on either cable 2 or cable 3 using the heaters. Similar data is plotted in figure 9 for a ramp rate of 2000 A s^{-1}. Since it takes some time to initiate the quench, the heater is fired at a lower current during the faster ramp. For both ramp rates, the Hall signals detect the onset of a quench before or as soon as a detectable voltage is measured over any of the cables in the triplet. This is clearer in figure 10, where the derivatives of both the Hall sensor voltage, as well as the voltage contact data are plot together on the same scale. This is a good way to compare the temporal response of the two quench detection methods since it shows their relative sensitivity in mV/A. It also highlights the additional noise that appears in the voltage measured over the terminations since the voltage wires form a larger inductive pickup loop than for the individual cable voltage measurements.

4. Discussion

A large signal can be measured with the Hall sensors concurrent with the first detectable voltage rise across the sample due to a hotspot using the same data acquisition (DAQ), and with no additional signal conditioning or amplification. For measurements on longer samples such as coils, the noise floor in the voltage contact measurements is expected to increase significantly while that of the Hall sensors will likely remain the same, allowing them to detect the development of a hotspot well before voltage tap measurements. In a fusion device, this additional time is valuable to de-energize magnets prior to thermal runaway and protect against potential magnet burn-out. Another important benefit of Hall sensor arrays is that the measurement is performed locally, near the cable termination, instead of requiring voltage wires to be co-wound with the cable. Hall sensors could be readily replaced in case of failure, while it is almost impossible to replace or repair a broken voltage wire that's co-wound with the magnet windings.

Placing Hall sensors between cables in the CORC® triplet is advantageous because the self-field of cables on either side tends to cancel out. This is demonstrated by the Biot-Savart calculations presented in figure 11, where the magnetic field distribution due to the triplet's self-field is calculated by adding the contributions of each cable. The calculations were validated by comparing to Finite Element modeling performed in Opera. Three cases are presented. In figure 11(a), the case is presented where each cable carries a current of 1 kA, representing normal triplet operation at about 75% of I_c. In figure 11(b), the current in the middle cable (cable 2) is reduced to 600 A while keeping the total current constant by

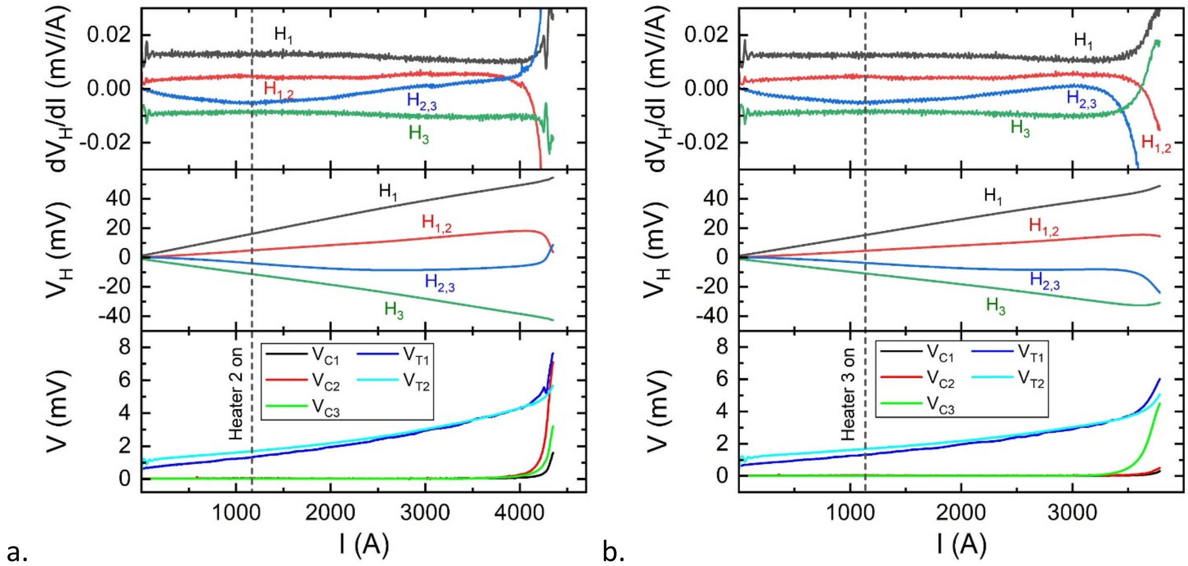

Figure 9. CORC® sample voltages (bottom), Hall voltages (middle), and derivative of Hall voltages (top) as a function of current measured at 76 K at a current ramp rate of 2000 A s^{-1} while a hotspot is initiated by applying a heater to (a) cable 2 and (b) cable 3.

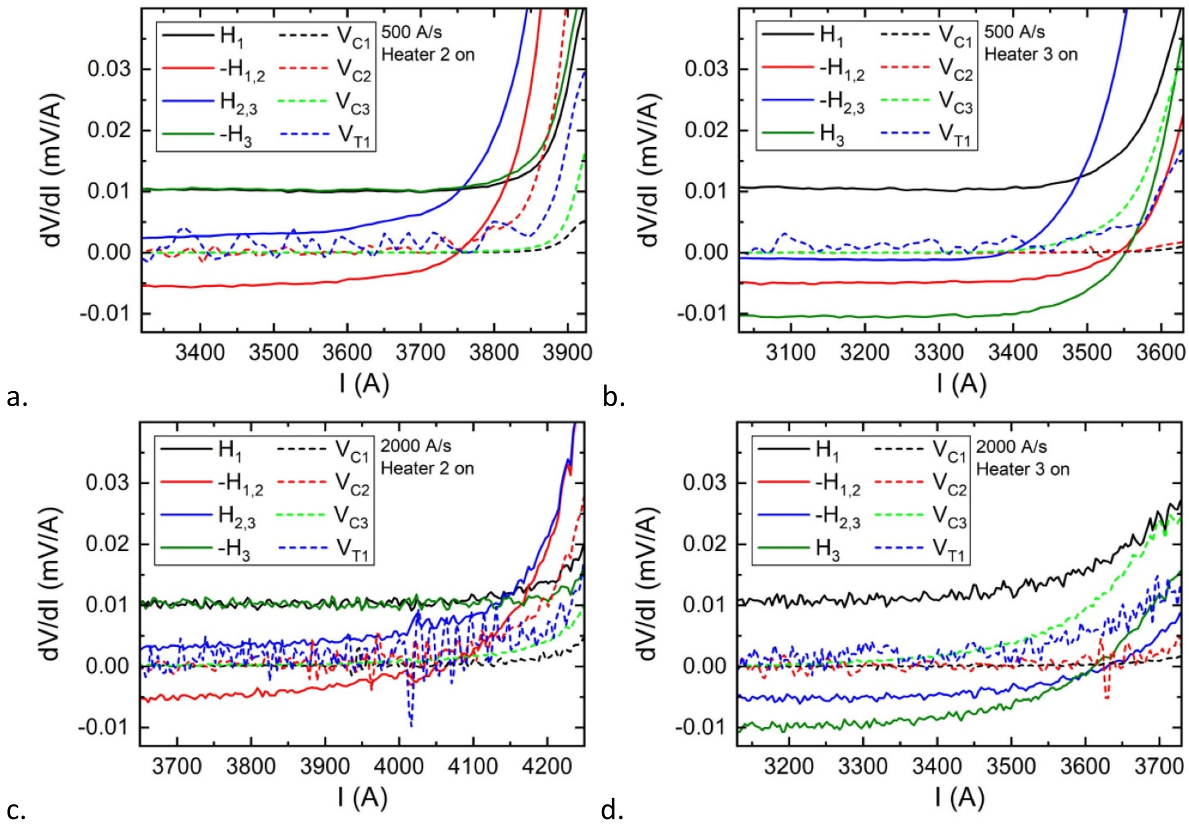

Figure 10. Comparison of CORC® Hall sensor (solid lines) and voltage tap (dashed lines) responses at 76 K as a function of current during current ramping, with 5 W heater applied to (a) cable 2 at 500 A s^{-1}, (b) cable 3 at 500 A s^{-1}, (c) cable 2 at 2000 A s^{-1}, and (d) cable 3 at 2000 A s^{-1}. For a clear comparison, Hall voltage responses are always shown to trend towards a positive value as the cables quench.

routing the excess current to the outer cables. This is similar to the experiment shown in figures 5(a) and (b) where a hotspot was initiated in the central cable at a total operating current of 3 kA. Similarly, figure 11 shows the case where current is reduced to 600 A in cable 3, reminiscent of the experiment in figures 5(c) and (d). Although the triplet sample allowed placement of Hall probes between the cables, initial modeling has shown that Hall probes would also be able to detect minute changes in current distribution in a 6-around-1 CICC, where the Hall probes are placed around the bundle of cables. These

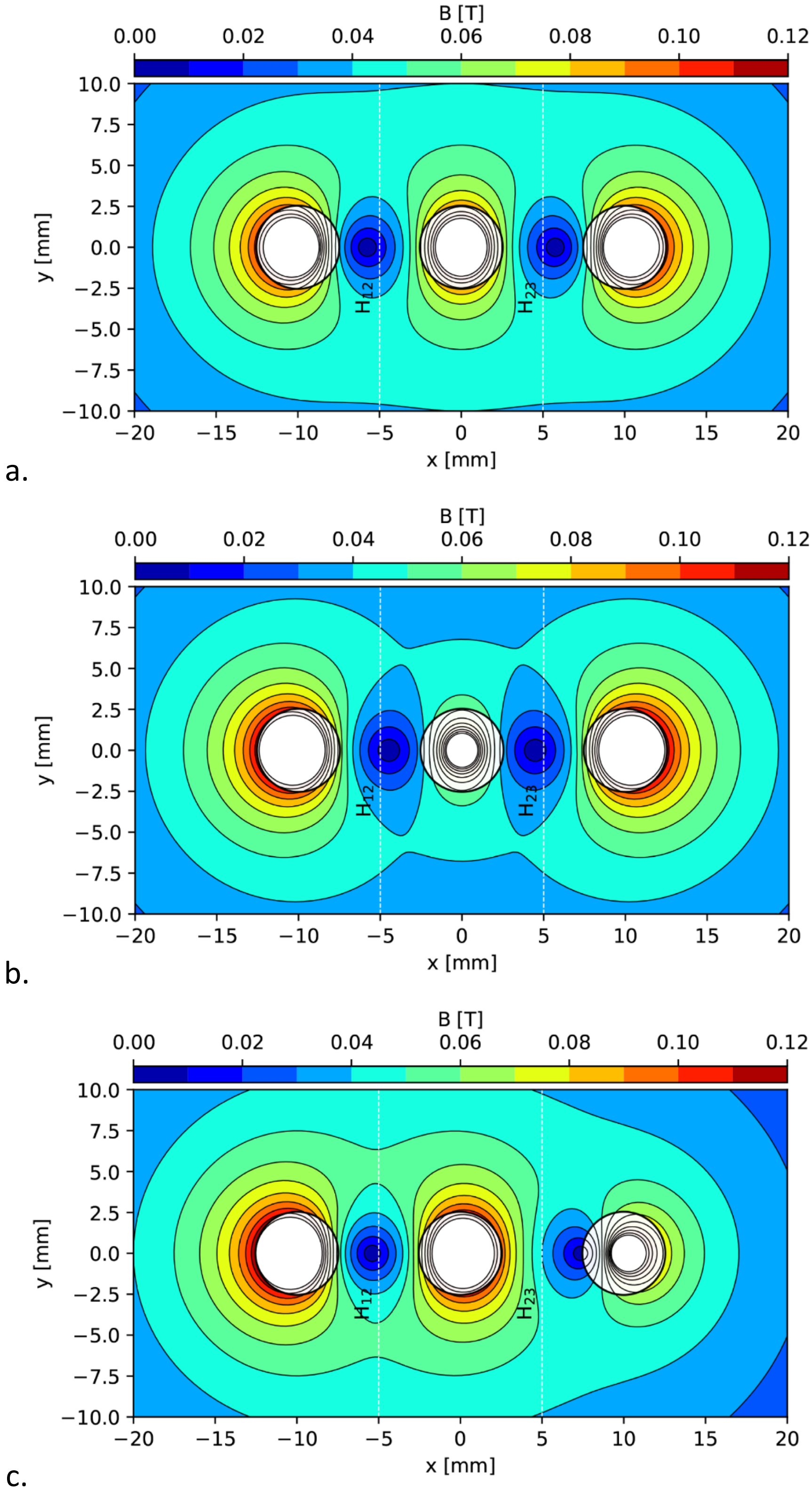

Figure 11. Magnetic flux density contours around the CORC® triplet calculated for (a) normal operation at 1 kA per cable, (b) the case where 400 A is redistributed from cable 2 to cables 1 and 3, and (c) where 400 A is redistributed from cable 3 to cables 1 and 2. Dashed lines at x = − 5 and x = 5 mm show the location of Hall sensors $H_{1,2}$ and $H_{2,3}$.

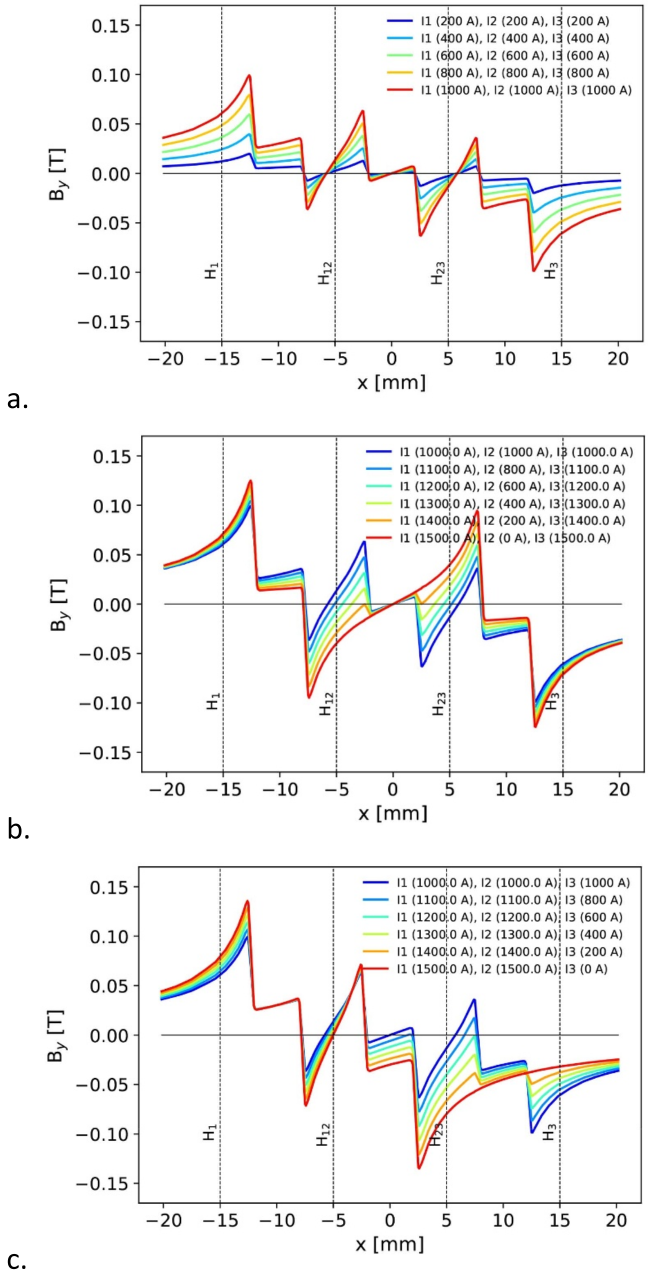

Figure 12. Vertical component of magnetic flux density as a function of position through the midplane of CORC® triplet at various operating currents with (a) even current distribution between cables (b) case where cable 2 is quenched, and (c) case where cable 3 is quenched, while overall current is kept constant. Dashed lines show the locations of the Hall sensors.

results and their experimental verification will be published elsewhere.

Figure 12(a) shows the calculated magnetic field perpendicular to the cable plane (B_y) through the midplane of the CORC® triplet with respect to the placement of the Hall sensors at various operating currents when current is distributed evenly between cables. Figure 12(b) shows how the field profile changes as current is redistributed from cable 2 into the other two cables while keeping the total current constant due to a normal zone developing. Similarly, figure 12(c) shows how the field profile changes as current is redistributed from cable 3. Another way to show this data is to plot B_y as a function of the reduced current in cable 2 (ΔI_2) or cable 3 (ΔI_3) for each sensor location (figures 13(a) and (b). When starting from the left of the plots ($I_1 = I_2 = I_3 = 1000$ A) and then moving to the right (increasing ΔI), the trends show the expected Hall sensor response of the experiments shown in figures 6(a) and 7(a), as current is reduced in cable 2 or cable 3, respectively.

In figure 6, the difference in Hall sensor voltage (ΔV_H) for sensors $H_{1,2}$ and $H_{2,3}$ was ± 50 μV before any voltage was measured using the voltage contacts. Considering the approximate transfer function of the Hall sensors used for the CORC® triplet of about 0.36 mV mT^{-1} at room temperature,

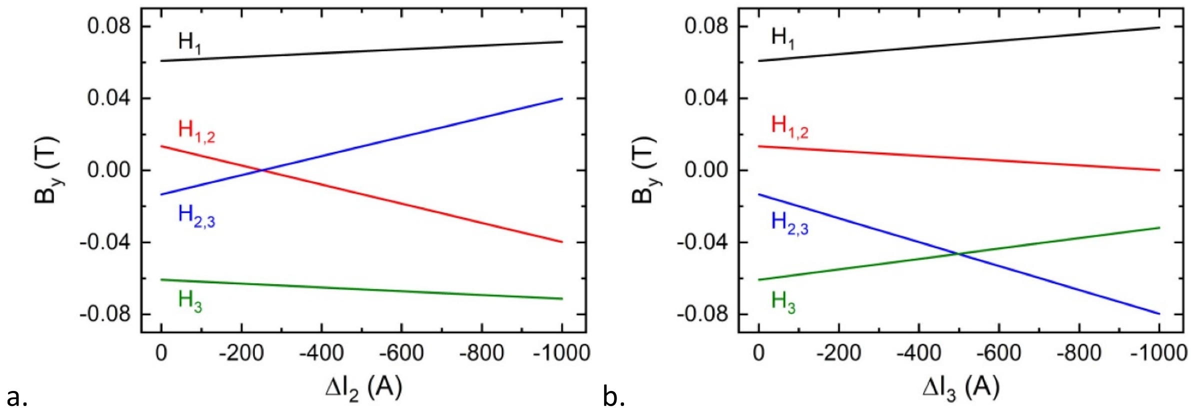

Figure 13. Magnetic flux density at each Hall sensor location taken from figure 12 as a function of reduced current of (a) cable 2 or (b) cable 3, while keeping the total current constant.

$\Delta V_H = 50\ \mu V$ corresponds to only 0.14 mT. The slope of the response of Hall sensors $H_{1,2}$ and $H_{2,3}$ from figure 13(a) is ± 0.05 mT A^{-1}, meaning we were able to clearly measure the effect of current redistribution of just 3 A, or only 0.1% of the operating current, at the onset of a hotspot causing a voltage to develop locally over cable 2 that was below the resolution of our voltage contact measurements. The peak ΔV_H measured during the heat-pulse experiment in figure 5(a) using Hall sensors $H_{1,2}$ and $H_{2,3}$ was about 10 mV, corresponding to approximately 750 A in cable 2, while the remaining 2250 A was divided between cables 1 and 3.

In figure 7, ΔV_H for Hall sensors $H_{2,3}$ was $-50\ \mu V$ at the same time that 10 μV (0.2 $\mu V\ cm^{-1}$) was measured with the voltage contacts over cable 3, while no voltage was detectable over cables 1 and 2. The slope of the response of Hall sensor $H_{2,3}$ from figure 13(b) is 0.07 mT A^{-1}, meaning we were able to clearly measure the effect of current redistribution of just 2 A as cable 3 barely exceeded I_c. A voltage of 10 μV does not develop over cable 2 until ΔV_H of Hall sensor $H_{2,3}$ was about 5 mV, corresponding to approximately 800 A in cable 3. Cable 1 only just started to develop voltage after the heater was switched off at a ΔV_H of 10 mV measured with Hall sensor $H_{2,3}$.

LTS superconducting magnets often quench while their currents are ramped due to additional dissipation associated with AC losses or conductor movement under Lorentz forces. In fusion machines, dynamic poloidal and central solenoidal fields are required, meaning conductors need to be ramped rapidly and often. For this reason, it is pertinent that quench detection approaches take ramping current conditions into account. For the dynamic measurements presented in figures 9 and 10, the Hall sensors proved to be effective at measuring current redistribution due to the heater-induced normal zone that developed well before the cables reached their I_c.

Variation of inductance or differences in AC loss between different cables in CICC could cause current imbalance for sufficiently long conductors at high ramp rates. While cables in the CORC® triplet were separated, effectively eliminating current sharing between cables, the contact resistance between cables installed in a copper jacket, for instance, could provide a path for current to redistribute outside the terminations. The contact resistance between CORC® cables within the CICC could be increased if needed to reduce current sharing between cables, as is done for ITER conductors in which metal foils limit current sharing between sub-cables to decrease coupling losses [43]. Another option to minimize differences in strand inductance would be to use the technique for quench detection in demountable TF coils, where each magnet turn is broken up into short sections of CICC with the sub-cables shorted at the joints.

Local current sensing has been demonstrated in LTS CICC using Hall sensors and pickup coils [33, 34]. Current nonuniformities have been observed, particularly in ramping conditions, that have been attributed to conductor movement and/or large induced current loops, but not necessarily due to quench. We expect these phenomena to be absent or less pronounced in HTS coils that benefit from higher thermal stability. Scale-up of the quench detection technique to longer coils may therefore be more viable for protecting HTS magnet systems since LTS magnets can be more susceptible to current redistribution from other sources.

The quench experiments (ex. Figure 5) performed on the CORC® triplet and the simulations shown in figure 11 highlight a key advantage of using Hall sensor arrays not only for quench detection, but for diagnostics as well. Current redistribution, or uneven current distribution between CORC® cables, is immediately measurable and the cable(s) affected can be identified. This requires very little instrumentation and wiring, as a relatively small array consisting of 1 sensor per sub-cable can be used. Sensors do not have to be placed between sub-cables as demonstrated here but could be arranged at other strategic locations within or around a CICC, as the self-field of the sub-cables is significant for high-current conductors. Such optimizations are an area of future work. One could also consider connecting the output of sensor pairs on either side of each sub-cable using a differential amplifier such that their voltages cancel out in normal operation but are amplified when there is a current imbalance. This configuration would result in a signal only when current flows unevenly between cables. It would also eliminate errors due to common mode background fields within a fusion device and could be used directly to trigger quench protection hardware.

5. Conclusion

The effectiveness of using Hall sensors to measure current redistribution between cables and detect the onset of a quench in a CORC® triplet was determined in liquid nitrogen. The Hall sensor voltages were compared to voltages measured over each cable with voltage wires as a normal zone developed within one of the cables due to a heater-induced hotspot for both constant current and ramping current conditions. Uneven current distribution was measured with the Hall sensors during current ramping at the onset of any measurable resistance. It was determined both experimentally and numerically that the magnetic field distribution around cables in the triplet changes significantly when current is redistributed between cables due to formation of a hotspot. The resolution of the Hall sensors was high enough to identify current redistribution on the order of a few amperes for a triplet carrying several kilo-amperes of current, or about 0.1% of the operating current. A hotspot that developed in one of the cables could be identified when current redistributed to the other cables in the triplet, well before a detectable voltage developed over the cable. Furthermore, an array of Hall sensors enabled active monitoring of current distribution between cables and will therefore be a valuable diagnostic tool for assessing the quality of terminations and joints in, for instance, demountable TF coils. Quench detection using Hall sensors located at the terminations of CORC®-CICC is a highly valuable method that can potentially detect the formation of a hotspot deep within a winding, at a far distance away from the sensor. While future tests on longer cables are warranted, the results demonstrate the value of this low-cost and easily implemented methodology for both quench detection and probing current dynamics in future HTS magnets being developed for fusion and other applications.

Acknowledgments

This work was supported in part by the US Department of Energy under contract numbers DE-SC0014009 and DE-SC0019934.

ORCID iDs

J D Weiss https://orcid.org/0000-0003-0026-3049
R Teyber https://orcid.org/0000-0001-6924-4175
M Marchevsky https://orcid.org/0000-0001-7283-9305
D C van der Laan https://orcid.org/0000-0001-5889-3751

References

[1] Bruzzone P *et al* 2018 High temperature superconductors for fusion magnets *Nucl. Fusion* **58** 103001
[2] Whyte D G, Minervini J, LaBombard B, Marmar E, Bromberg L and Greenwald M 2016 Smaller & sooner: exploiting high magnetic fields from new superconductors for a more attractive fusion energy development path *Springer US* Jan Accessed: Apr 19 2020 [Online] available: https://dspace.mit.edu/handle/1721.1/105878
[3] Zhai Y, Titus P, Kessel C and El-Guebaly L 2018 Conceptual magnet design study for fusion nuclear science facility *Fusion Eng. Des.* **135** 324–36
[4] Gourlay S A 2018 Superconducting accelerator magnet technology in the 21st century: A new paradigm on the horizon? *Nucl. Instrum. Methods Phys. Res. Sect.* **893** 124–37
[5] Rossi L *et al* 2018 The EuCARD2 future magnets program for particle accelerator high-field dipoles: review of results and next steps *IEEE Trans. Appl. Supercond.* **28** 3
[6] Zohm H 2019 On the use of high magnetic field in reactor grade tokamaks *J. Fusion Energy* **38**3–10
[7] Uglietti D 2019 A review of commercial high temperature superconducting materials for large magnets: from wires and tapes to cables and conductors *Supercond. Sci. Technol.* **32** 5
[8] Sorbom B N *et al* 2015.ARC: A compact, high-field, fusion nuclear science facility and demonstration power plant with demountable magnets *Fusion Eng. Des.* **100** 378–405
[9] Yanagi N *et al* 2015.Design and development of high-temperature superconducting magnet system with joint-winding for the helical fusion reactor *Nucl. Fusion* **55** 053021
[10] van der Laan D C, Weiss J D and McRae D M 2019 Status of CORC® cables and wires for use in high-field magnets and power systems a decade after their introduction *Supercond. Sci. Technol.* **32** 3
[11] van der Laan D C, Noyes P D, Miller G E, Weijers H W and Willering G P 2013 Characterization of a high-temperature superconducting conductor on round core cables in magnetic fields up to 20 T *Supercond. Sci. Technol.* **26** 4
[12] van der Laan D C *et al* 2016.Record current density of 344 A mm^{-2} at 4.2 K and 17 T in CORC® accelerator magnet cables *Supercond. Sci. Technol.* **29** 5
[13] Takayasu M, Chiesa L, Bromberg L and Minervini J V 2011 Cabling method for high current conductors made of HTS tapes *IEEE Trans. Appl. Supercond.* **21** 3
[14] Takayasu M, Mangiarotti F J, Chiesa L, Bromberg L and Minervini J V 2013 Conductor characterization of YBCO twisted stacked-tape cables *IEEE Trans. Appl. Supercond.* **23** 3
[15] Goldacker W, Grilli F, Pardo E, Kario A, Schlachter S I and Vojenčiak M 2014 Roebel cables from REBCO coated conductors: a one-century-old concept for the superconductivity of the future *Supercond. Sci. Technol.* **27** 9
[16] Uglietti D, Bykovsky N, Sedlak K, Stepanov B, Wesche R and Bruzzone P 2015 Test of 60 kA coated conductor cable prototypes for fusion magnets *Supercond. Sci. Technol.* **28** 12
[17] Uglietti D, Wesche R and Bruzzone P 2014 Design and strand tests of a fusion cable composed of coated conductor tapes *IEEE Trans. Appl. Supercond.* **24** 3
[18] Augieri A *et al* 2015 Electrical characterization of ENEA high temperature superconducting cable *IEEE Trans. Appl. Supercond.* **25** 3

[19] Celentano G *et al* 2014 Design of an industrially feasible twisted-stack HTS cable-in-conduit conductor for fusion application *IEEE Trans. Appl. Supercond.* **24** 4601805
[20] Wolf M J, Fietz W H, Bayer C M, Schlachter S I, Heller R and Weiss K 2016 HTS CroCo: A stacked HTS conductor optimized for high currents and long-length production *IEEE Trans. Appl. Supercond.* **26** 2
[21] Wolf M J, Bagrets N, Fietz W H, Lange C and Weiss K-P 2018 Critical current densities of 482 A/mm^2 in HTS crossConductors at 4.2 kelvin and 12 tesla *IEEE Trans. Appl. Supercond.* **28** 4802404
[22] Terazaki Y *et al* 2015 Measurement and analysis of critical current of 100-kA class simply-stacked HTS conductors *IEEE Trans. Appl. Supercond.* **25** 4602905
[23] Mulder T, Weiss J, Van Der Laan D, Dudarev A and and Ten Kate H 2020 Recent progress in the development of CORC® cable-in-conduit conductors *IEEE Trans. Appl. Supercond.* **30** 4800605
[24] Mulder T *et al* 2016 Design and manufacturing of a 45 kA at 10 T REBCO-CORC® cable-in-conduit conductor for large-scale magnets *IEEE Trans. Appl. Supercond.* **26** 4
[25] Song H and Schwartz J 2009 Stability and quench behavior of $YBa_2Cu_3O_{7-x}$ coated conductor at 4.2 K, self-field *IEEE Trans. Appl. Supercond.* **19** 3735–43
[26] Wang X, Trociewitz U P and Schwartz J 2009 Self-field quench behaviour of $YBa_2Cu_3O_{7-\delta}$coated conductors with different stabilizers *Supercond. Sci. Technol.* **22** 085005
[27] Senatore C, Alessandrini M, Lucarelli A, Tediosi R, Uglietti D and Iwasa Y 2014 Progresses and challenges in the development of high-field solenoidal magnets based on RE123 coated conductors *Supercond. Sci. Technol.* **27** 103001
[28] Scurti F, Ishmael S, Flanagan G and Schwartz J 2016 Quench detection for high temperature superconductor magnets: a novel technique based on Rayleigh-backscattering interrogated optical fibers *Supercond. Sci. Technol.* **29** 03LT01
[29] van der Laan D C, Weiss J D, Scurti F and Schwartz J 2020 CORC® wires with integrated optical fibers for temperature and strain monitoring and voltage wires for reliable quench detection *Supercond. Sci. Technol.* **33** 085010
[30] Ravaioli E, Martchevskii M, Sabbi G, Shen T and Zhang K 2018 Quench detection utilizing stray capacitances *IEEE Trans. Appl. Supercond.* **28** 4702805
[31] Marchevsky M, Hershkovitz E, Wang X, Gourlay S A and Prestemon S 2018 Quench detection for high-temperature superconductor conductors using acoustic thermometry *IEEE Trans. Appl. Supercond.* **28** 4
[32] Lenz J E 1990 A review of magnetic sensors *Proc. IEEE* **78** 973–89
[33] Vysotsky V S, Takayasu M, Ferri M, Minervini J V and Shen S S 1995 New method of current distribution studies for ramp rate stability of multistrand superconducting cables *IEEE Trans. Appl. Supercond.* **5** 580–3
[34] Balsamo E P *et al* 2000 Experimental study of the current redistribution in pulsed operation inside the Nb/sub 3/Sn CICC of an ITER relevant magnet *IEEE Trans. Appl. Supercond.* **10** 1598–602
[35] Marchevsky M, Xie -Y-Y and Selvamanickam V 2010 Quench detection method for 2G HTS wire *Supercond. Sci. Technol.* **23** 034016
[36] Teyber R, Marchevsky M, Prestemon S, Weiss J and van der Laan D 2020 CORC® cable terminations with integrated hall arrays for quench detection *Supercond. Sci. Technol.* **33** 095009
[37] Marchevsky M, Prestemon S, van der Laan D C and Weiss J D 2020Imaging current sharing and quench propagation in a high T_c superconducting CORC cable using Hall sensor array *Supercond. Sci. Technol.* Under review
[38] Willering G P' van der Laan D C' Weijers H W' Noyes P D' Miller G E and Viouchkov Y 2015 Effect of variations in terminal contact resistances on the current distribution in high-temperature superconducting cables *Supercond. Sci. Technol.* **28** 3
[39] Mulder T' Dudarev A' Mentink M' Silva H and van der Laan D 2016 Development of joint terminals for a new six-around-one ReBCO-CORC® cable-in-conduit conductor rated 45 kA at 10 T/4 K *IEEE Trans. Appl. Supercond.* **26** 3
[40] Mulder T *et al* 2017 Demonstration of the ReBCO CORC® 47kA@10T/4.2K cable-in-conduit-conductor and its joint terminals at 4.5 and 77 K *IEEE Trans. Appl. Supercond.* **27** 4
[41] Bykovsky N, Uglietti D, Sedlak K, Stepanov B, Wesche R and Bruzzone P 2016 Performance evolution of 60 kA HTS cable prototypes in the EDIPO test facility *Supercond. Sci. Technol.* **29** 8
[42] Yagotintsev K A, Anvar V A, Gao P, Dhalle M J, Haugan T J, Van Der Laan D C, Weiss J D, Hossain M S A and Nijhuis A 2020AC loss and contact resistance in REBCO, CORC, Roebel, and stacked tape cables *Supercond. Sci. Technol. Rev.* **33** 085009
[43] Nijhuis A, Ilyin Y, Abbas W, Ten Haken B and Ten Kate H H J 2004 Change of interstrand contact resistance and coupling loss in various prototype ITER NbTi conductors with transverse loading in the twente cryogenic cable press up to 40,000 cycles *Cryogenics* **44** 319–39
[44] Yagotintsev K A *et al* 2019.Overview of verification tests on AC loss, contact resistance and mechanical properties of ITER conductors with transverse loading up to 30 000 cycles *Supercond. Sci. Technol.* **32** 105015